MATCH
Communications in Mathematical and in Computer Chemistry

MATCH Commun. Math. Comput. Chem. **90** (2023) 19–51
ISSN: 0340–6253
doi: 10.46793/match.90-1.019A

Statistical Analysis of a General Adsorption Kinetic Model with Randomness in Its Formulation. An Application to Real Data

Carlos Andreu–Vilarroig[a], Juan-Carlos Cortés[a,*], Ana Navarro–Quiles[b], Sorina–Madalina Sferle[a]

[a] *Instituto Universitario de Matemática Multidisciplinar, Universitat Politècnica de València, Camino de Vera s/n, 46022, Valencia, Spain.*

[b] *Department of Statistics and Operational Research, Universitat de València, Dr. Moliner 50, 46100, Burjassot, Spain.*

caranvi1@etsii.upv.es, jccortes@imm.upv.es, ana.navarro@uv.es, smsferle@doctor.upv.es

(Received July 14, 2022)

Abstract

The general adsorption kinetic model, also called pseudo-n orden (PNO) equation, is revisited using random differential equations. We provide a full probabilistic solution of the model, which is a stochastic process, by computing its first probability density function under very general hypotheses on its parameters, that are treated as absolutely continuous random variables with an arbitrary joint probability density function. The analysis is based on the so called Random Variable Transformation technique. From the first probability density function, we compute relevant information of the PNO model, such that, the mean, the variance and confidence interval. We also provide explicit expressions for the probability density functions of other significant quantities as the time required to reach a specific level of absorbed substance or the rate coefficient of the

*Corresponding author.

chemical reaction. All the theoretical findings are illustrated by means of real data. The application includes a thorough discussion about two important uncertainty quantification inverse methods, namely, the Random Least Mean Square and the Bayesian technique, to assign appropriate probability density functions to all the PNO model parameters so that the solution captures data uncertainties.

1 Preliminaries

One of the most studied phenomena in the world of chemistry is adsorption. Adsorption is a surface accumulation process, in which a substance (the adsorbate) interacts and binds to another substance (the adsorbent or substrate) on a surface [6]. Within the adsorption processes, we can find physisorption, in which molecules interact by intermolecular (Van del Waals) forces and chemisorption, in which molecules bind by chemical reactions. Of these two processes, chemisorption is the more energy-intensive process because of the types of bonds formed between molecules (covalent or ionic) [27]. Since the beginning of the study of adsorption, several mathematical models - both empirical and based on physical principles - have been proposed [31, 37]. Initially, these models were focused on explaining both the adsorbate/adsorbent equilibrium of the process at constant temperature, the so-called adsorption isotherm. In this way, Langmuir's isotherm model [19] has had the greatest impact, and more complex isotherm models (Sips, Redlich–Peterson, etc.) have followed it [22]. Nevertheless, the emergence of new chemisorption applications, such as water and wastewater treatment processes [2,7–9,38], and new technical advances in spectroscopy or electron microscopy, which have made it possible to analyse the adsorption phenomenon at molecular level [11, 20, 24, 30, 36], leads to adsorption kinetics models, which focus especially on the reaction pathways and mechanisms [22].

Traditionally, the most commonly used models in adsorption kinetics have been the Lagergren or pseudo-first order (PFO) and the pseudo-

second order (PSO) models [13, 18], given by the equations

$$\text{PFO:} \quad \frac{\mathrm{d}q(t)}{\mathrm{d}t} = k_1(q_\mathrm{e} - q(t)),$$
$$\text{PSO:} \quad \frac{\mathrm{d}q(t)}{\mathrm{d}t} = k_2(q_\mathrm{e} - q(t))^2,$$

where $q_\mathrm{e} \in \mathbb{R}_{>0}$ is the adsorption capacity at equilibrium (mg/g), $q(t)$ the adsorption capacity at time t (mg/g) and k_1 (min^{-1}) and k_2 ($(\mathrm{mg/g})^{-1}$ min^{-1}) the adsorption rates [†]. Other usual model, that can be found in the literature, is the (empirical) Elovich equation [23], defined as

$$\text{Elovich:} \quad \frac{\mathrm{d}q(t)}{\mathrm{d}t} = ae^{-bq(t)},$$

where a ($(\mathrm{mg/g})$ min^{-1}) and b ($(\mathrm{mg/g})^{-1}$) are empirical parameters. As can be seen from the equations, the factor that causes adsorption to decrease and brings the equations closer to equilibrium is the amount adsorbed $q(t)$. Physically, this is related to the free space remaining on the surface at each instant of time, and which has been occupied by a quantity $q(t)$: the greater the amount adsorbed, the less space available, and the less adsorption will occur. All these models have been extensively applied, see for instance [1, 4, 5, 21, 25, 26, 29, 38].

In 1977, the Ritchie model was published as a generalised equation of the previous models, and in response to the limitations that other models, such as the Elovich equation, presented when applied to certain experiments [32]. Ritchie's model is given by the equation

$$\text{Ritchie:} \quad \frac{\mathrm{d}\theta(t)}{\mathrm{d}t} = \lambda(1 - \theta(t))^n, \tag{1}$$

where θ is the fraction of surface area occupied by the adsorbate and λ is the adsorption rate (min^{-1}). If the adsorbed quantity $q(t)$ is introduced, Ritchie's equation is transformed into the pseudo-n order (PNO) equation

[†]The units of the quantities q in mg/g represent milligrams of adsorbate per gram of adsorbent.

[28] (see the complete proof in Appendix A), given by

$$\frac{\mathrm{d}q(t)}{\mathrm{d}t} = k_n(q_\mathrm{e} - q(t))^n, \tag{2}$$

$$k_n = \frac{\lambda}{q_\mathrm{e}^{n-1}}, \tag{3}$$

where k_n is the rate coefficient ($(\mathrm{mg/g})^{-n+1}$ min^{-1}) and n is the order of the reaction, which is physically equivalent to the number of binding sites that an adsorbate molecule occupies when binding to the surface. By integrating the equation, the exact solution of the PNO model is obtained

$$q(t) = \begin{cases} q_\mathrm{e}\left(1 - e^{-k_1 t}\right) & \text{if } n = 1, \\ q_\mathrm{e} - q_\mathrm{e}\left(\frac{1}{1+(n-1)q_\mathrm{e}^{n-1}k_n t}\right)^{\frac{1}{n-1}} & \text{if } n > 1, \end{cases} \tag{4}$$

and substituting k_n for its expression, indicated in (3),

$$q(t) = \begin{cases} q_\mathrm{e}\left(1 - e^{-\lambda t}\right) & \text{if } n = 1, \\ q_\mathrm{e} - q_\mathrm{e}\left(\frac{1}{1+(n-1)\lambda t}\right)^{\frac{1}{n-1}} & \text{if } n > 1. \end{cases} \tag{5}$$

From the physical and mathematical analysis of the model, it can be stated that $\lambda \in \mathbb{R}_{>0}$, $q_\mathrm{e} \in \mathbb{R}_{>0}$ and $n \in \mathbb{R}_{\geq 1}$ (see the justification in Appendix B).

Classically, the kinetic parameters are deduced by fitting the experimental data with the model equations of the model considered, by linearising equations or by applying numerical methods, usually Runge-Kutta method [37]. This approach entails calibrating the model by means of deterministic constants that may lead, in some cases, to inadequate model calibration, particularly when the chemical process is affected by different sources of uncertainty (e.g., errors in the experimental data). Also, the adsorption process at the molecular level has an intrinsic randomness by its own nature, and there are experimental physico-chemical conditions such as pressure, concentrations, pH, etc. (some of which are difficult to control) that can significantly alter the results if they are modified between experiments. On the other hand, new advances in statistical techniques for

the treatment of uncertainty in mathematical modelling, especially in the field of differential equations, make it possible to treat so far deterministic models as random differential equations. In this way, the solutions to the differential equations are no longer classical or deterministic functions and become stochastic processes with their corresponding associate probability distributions. Recently, this stochastic approach has already started to be applied to the PNO model in [33], by introducing a term that represents the randomness of the adsorption process.

It is important to take this uncertainty into account from the very beginning of the model. There are several ways to introduce uncertainties into model formulation. On the one hand, by means of a stationary and Gaussian stochastic process, called white noise, that is the derivative (in the sense of distributions or generalized functions) of the Wiener stochastic process (also termed Brownian motion). This way of considering uncertainties in differential equations leads to the so called Stochastic Differential Equations (SDEs) [3]. On the other hand, uncertainties can be alternative introduced in differential equations by directly treating the model parameters as random variables or stochastic processes. This approach leads to Random Differential Equations (RDEs). Unlike the SDEs approach, RDEs allow us to consider wider range of random patterns to be introduced in the model formulation, since many probability distributions can be considered, apart from the Gaussian one [35]. This is a key fact that confer RDEs more flexibility in real-world applications [34].

Our proposed randomised PNO model is given by

$$q(t,\omega) = \begin{cases} q_{\mathrm{e}}(\omega)\left(1-\mathrm{e}^{-\lambda(\omega)t}\right) & \text{if } n(\omega)=1, \quad \omega\in\Omega, \\ q_{\mathrm{e}}(\omega)-q_{\mathrm{e}}(\omega)\left(\frac{1}{1+(n(\omega)-1)\lambda(\omega)t}\right)^{\frac{1}{n(\omega)-1}} & \text{if } n(\omega)>1, \quad \omega\in\Omega, \end{cases} \tag{6}$$

where the adsorption rate, or rate coefficient, $\lambda(\omega)$, the adsorbed amount at equilibrium, $q_{\mathrm{e}}(\omega)$, and the order of the kinetic model, $n(\omega)$, are assumed to be absolutely continuous random variables defined on a common complete probability space $(\Omega, \mathcal{F}_\Omega, \mathbb{P})$. It also should be noted that, as in the deterministic model, q_{e}, $\lambda \in \mathbb{R}_{>0}$ and $n \in \mathbb{R}_{\geq 1}$, so in the random

scenario we need consider random variables with the same domain. As a punctual modification, since the probability that $n(\omega) = 1$, being a continuous variable, is 0, we will study only the case in which $n(\omega) > 1$, i.e., $n \in \mathbb{R}_{>1}$. Hereinafter, we will denote by $\mathcal{D}_{\lambda,q_e,n} \subset \mathbb{R}^3_{>0}$ the domain of the random vector $(\lambda(\omega), q_e(\omega), n(\omega))$, since each model parameter must be positive.

From a general perspective, the three random variables are characterised by a joint probability density function (PDF) $f_0(\lambda, q_e, n)$. In case of independence, the joint PDF can be computed as the product of the marginals, $f_0(\lambda, q_e, n) = f_\lambda(\lambda) f_{q_e}(q_e) f_n(n)$. In order to provide a complete probabilistic description of the solution, $q = q(t)$, at each time instant, the main goal is to find its first probability density function (1-PDF), denoted by $f_1(q,t)$. Then, by integrating the 1-PDF, all the one-dimensional statistical moments of $q(t,\omega)$, such as the mean and the variance, can be computed. Formally,

$$\begin{aligned} &\mathbb{E}\left[q(t,\omega)^s\right] = \int_{\mathbb{R}} q^s f_1(q,t)\,\mathrm{d}q, \quad s = 1,2,\dots \\ &\begin{cases} \mu_q(t) &= \mathbb{E}\left[q(t,\omega)\right] = \int_{\mathbb{R}} q f_1(q,t)\,\mathrm{d}q, \\ \sigma_q^2(t) &= \mathbb{V}\left[q(t,\omega)\right] = \int_{\mathbb{R}} q^2 f_1(q,t)\,\mathrm{d}q - (\mu_q(t))^2. \end{cases} \end{aligned} \tag{7}$$

In addition, the 1-PDF also allows us to calculate the probability that the solution lies within a particular interval of interest, say $[a,b]$, given a fixed time instant t,

$$\mathbb{P}\left[\{\omega \in \Omega \,:\, a \le q(t,\omega) \le b\}\right] = \int_a^b f_1(q,t)\,\mathrm{d}q.$$

And, the probability that the adsorbed amount exceeds a given quantity $\hat{q}$,

$$\mathbb{P}\left[\{\omega \in \Omega \,:\, q(t,\omega) > \hat{q}\}\right] = \int_{\hat{q}}^{\infty} f_1(q,t)\,\mathrm{d}q.$$

The 1-PDF is also helpful to construct probabilistic intervals for any $(1-\alpha)\times 100\%$ confidence level. Namely, for $\alpha \in (0,1)$ and for each $\hat{t} \ge 0$ fixed,

the points that determine the probability of the interval can be determined by the following expression

$$\int_0^{q_1(\hat{t})} f_1(q,\hat{t})\,\mathrm{d}q = \frac{\alpha}{2} = \int_{q_2(\hat{t})}^1 f_1(q,\hat{t})\,\mathrm{d}q, \tag{8}$$

where

$$1-\alpha = \mathbb{P}\left[\{\omega\in\Omega\,:\,q(\hat{t},\omega)\in[q_1(\hat{t}),q_2(\hat{t})]\}\right] = \int_{q_1(\hat{t})}^{q_2(\hat{t})} f_1(q,\hat{t})\,\mathrm{d}q. \tag{9}$$

A common value is $\alpha = 0.05$, which means 95% confidence intervals.

As previously indicated, in this work we propose to study the PNO model of chemical adsorption considering its parameters as random variables. In Section 2 a complete analysis of the proposed model is carried out by determining the 1-PDF of the solution and the 1-PDF of the time needed to reach a particular level of adsorbed amount. In Section 3 the randomized PNO model is used to model the adsorption of cadmium onto ground-up tree fern [12], in order to test the theoretical model to real-world data. The application is carried out from two approaches: Randomized Least Mean Squares (RLMS) and Bayesian. The results and the comparison between both are also discussed in this Section. Finally, the conclusions of this study are drawn in Section 4.

2 Probabilistic solution

In this section, the 1-PDF of the solution of the general PNO model described in (6) is determined. Additionally, the PDF of the time needed to reach an arbitrary, but fixed, amount of adsorbent is calculated. To compute the density functions, we apply the Random Variable Transformation (RVT) technique. This method allows us to calculate the distribution of a random vector in terms of the known PDF of another random vector, provided that there is a one-to-one transformation between both random vectors. In Theorem 1, the multidimensional version of the RVT method is stated.

Theorem 1 (Random Variable Transformation technique [35]). *Let* $\mathbf{u}(\omega) = (u_1(\omega), \ldots, u_n(\omega))$ *and* $\mathbf{v}(\omega) = (v_1(\omega), \ldots, v_n(\omega))$ *be n-dimensional absolutely continuous random vectors. Let* $\mathbf{r} : \mathbb{R}^n \to \mathbb{R}^n$ *be a one-to-one transformation of* $\mathbf{u}$ *into* $\mathbf{v}$*, i.e.,* $\mathbf{v} = \mathbf{r}(\mathbf{u})$*. Assume that* $\mathbf{r}$ *is continuous in* $\mathbf{u}$ *and has continuous partial derivatives with respect to* $\mathbf{u}$*. Then, if* $f_{\mathbf{U}}(\mathbf{u})$ *denotes the joint PDF of the random vector* $\mathbf{u}(\omega)$*, and* $\mathbf{s} = \mathbf{r}^{-1} = (s_1(v_1, \ldots, v_n), \ldots, s_n(v_1, \ldots, v_n))$ *represents the inverse mapping of* $\mathbf{r} = (r_1(u_1, \ldots, u_n), \ldots, r_n(u_1, \ldots, u_n))$*, the joint PDF of vector* $\mathbf{v}(\omega)$ *is given by*

$$f_{\mathbf{V}}(\mathbf{v}) = f_{\mathbf{U}}\left(\mathbf{s}(\mathbf{v})\right) |J_n| \,,$$

where $|J_n|$ *is the absolute value of the Jacobian, which is defined by*

$$J_n = \det\left(\frac{\partial \mathbf{s}}{\partial \mathbf{v}}\right) = \det\begin{pmatrix} \dfrac{\partial s_1(v_1, \ldots, v_n)}{\partial v_1} & \cdots & \dfrac{\partial s_n(v_1, \ldots, v_n)}{\partial v_1} \\ \vdots & \ddots & \vdots \\ \dfrac{\partial s_1(v_1, \ldots, v_n)}{\partial v_n} & \cdots & \dfrac{\partial s_n(v_1, \ldots, v_n)}{\partial v_n} \end{pmatrix}.$$

2.1 1-PDF of the solution

Let $\mathbf{u}(\omega) = (\lambda(\omega), q_{\mathrm{e}}(\omega), n(\omega))$ be the random model parameters. Let $t > 0$ be a fixed value, and let us apply the RVT method to the following deterministic one-to-one transformation, $\mathbf{r} : \mathbb{R}^3 \to \mathbb{R}^3$, of $\mathbf{u}(\omega)$ into the random vector $\mathbf{v}(\omega) = (v_1(\omega), v_2(\omega), v_3(\omega))$, defined by

$$\begin{aligned} v_1 &= r_1(\lambda, q_{\mathrm{e}}, n) = q(t) = q_{\mathrm{e}} - q_{\mathrm{e}} \left(\frac{1}{1 + (n-1)\lambda t}\right)^{\frac{1}{n-1}}, \\ v_2 &= r_2(\lambda, q_{\mathrm{e}}, n) = q_{\mathrm{e}}, \\ v_3 &= r_3(\lambda, q_{\mathrm{e}}, n) = n. \end{aligned}$$

The inverse mapping $\mathbf{s} : \mathbb{R}^3 \to \mathbb{R}^3$ of $\mathbf{r}$ is obtained by isolating each $\mathbf{u}(\omega)$ component from each $\mathbf{v}(\omega) = (v_1(\omega), v_2(\omega), v_3(\omega))$ expression. This gives

$$\begin{aligned} \lambda = s_1(v_1, v_2, v_3) &= \frac{\left(1 - \frac{v_1}{v_2}\right)^{1-v_3} - 1}{t(v_3 - 1)}, \\ q_\mathrm{e} = s_2(v_1, v_2, v_3) &= v_2, \\ n = s_3(v_1, v_2, v_3) &= v_3. \end{aligned}$$

In the application of the RVT method, we shall check that the inverse mapping is well-defined, i.e., that the random parameters belong to its domain. In our case, knowing that $s_2 = v_2 = q_\mathrm{e} > 0$, $s_3 = v_3 = n > 1$ and $0 \leq \frac{v_1}{v_2} = \frac{q(t)}{q_\mathrm{e}} < 1$,

$$\left(1 - \frac{v_1}{v_2}\right)^{1-v_3} > 1 \implies s_1 = \lambda = \frac{\left(1 - \frac{v_1}{v_2}\right)^{1-v_3} - 1}{t(v_3 - 1)} > 0, \tag{10}$$

so it follows that the inverse mapping is well-defined in the conditional probability space $(\Omega, \mathcal{F}_\Omega, \mathbb{P}[\cdot|C])$, where $C = \{\omega \in \Omega : q_\mathrm{e}(\omega) > q(t, \omega)\}$. In this case, according to the given definition of $q(t, \omega)$, the event C is true $\forall\ \omega \in \Omega$, so its probability is $P[C] = 1$. Furthermore, the absolute value of its Jacobian of the inverse mapping $\mathbf{s}$ is given by

$$|J| = \frac{1}{tv_2\left(1 - \frac{v_1}{v_2}\right)^{v_3}} > 0.$$

Then, applying Th. 1, we obtain the PDF of the random vector $\mathbf{v}(\omega) = (v_1(\omega), v_2(\omega), v_3(\omega))$ in terms of the known joint PDF, f_0, of the random vector of the model parameters, $(\lambda(\omega), q_\mathrm{e}(\omega), n(\omega))$,

$$f_{v_1,v_2,v_3}(v_1, v_2, v_3) = f_0\left(\frac{\left(1 - \frac{v_1}{v_2}\right)^{1-v_3} - 1}{t(v_3 - 1)}, v_2, v_3\right) \frac{1}{tv_2\left(1 - \frac{v_1}{v_2}\right)^{v_3}}.$$

Finally, marginalising the last expression with respect to the random vector $(v_2(\omega), v_3(\omega)) = (q_\mathrm{e}(\omega), n(\omega))$, and letting $t > 0$ arbitrary, the 1-PDF of

the solution, $q(t,\omega)$, is

$$f_1(q,t) = \int_0^\infty \int_1^\infty f_0\left(\frac{\left(1-\frac{q}{q_e}\right)^{1-n}-1}{t(n-1)}, q_e, n\right) \frac{1}{tq_e\left(1-\frac{q}{q_e}\right)^n}\,\mathrm{d}n\,\mathrm{d}q_e, \tag{11}$$

defined in the conditional probability space $(\Omega, \mathcal{F}_\Omega, \mathbb{P}[\cdot|C]) = (\Omega, \mathcal{F}_\Omega, \mathbb{P}[\cdot])$.

In the case that $\lambda(\omega)$, $q_e(\omega)$ and $n(\omega)$ are independent random variables, the above expression can be expressed as

$$f_1(q,t) = \int_0^\infty \int_1^\infty f_\lambda\left(\frac{\left(1-\frac{q}{q_e}\right)^{1-n}-1}{t(n-1)}\right) f_{q_e}(q_e)\, f_n(n) \frac{1}{tq_e\left(1-\frac{q}{q_e}\right)^n}\,\mathrm{d}n\,\mathrm{d}q_e, \tag{12}$$

where f_λ, f_{q_e} and f_n denote the PDFs of $\lambda(\omega)$, $q_e(\omega)$ and $n(\omega)$, respectively.

2.2 PDF of time needed to reach an absorbed quantity

Given the random variables $\lambda(\omega), q_e(\omega), n(\omega) \in \mathcal{D}_{\lambda,q_e,n}$, the time t_ρ needed to adsorb a (deterministic) quantity $\rho > 0$ is deduced from (6):

$$t_\rho(\omega) = \frac{\left(1-\frac{\rho}{q_e(\omega)}\right)^{1-n(\omega)}-1}{\lambda(\omega)(n(\omega)-1)}, \quad \omega \in \Omega. \tag{13}$$

Observe that the random variable $t_\rho(\omega)$ is well-defined if and only if it is positive for each $\omega \in \Omega$. Then, from expression (13), $t_\rho(\omega)$ is defined in the conditional probability space $(\Omega, \mathcal{F}_\Omega, \mathbb{P}[\cdot|C])$, where $C = \{\omega \in \Omega : q_e(\omega) > \rho\} \in \mathcal{F}_\Omega$. Unlike in the other section, in this case as ρ is deterministic and fixed, $P[C]$ it is not necessarily one, therefore it shall be carefully considered in the computation of the PDF.

To obtain the PDF of $t_\rho(\omega)$, let us fix $\rho > 0$, and define the following mapping $\mathbf{r} : \mathbb{R}^3 \longrightarrow \mathbb{R}^3$ that transforms the random vector of model parameters $\mathbf{u}(\omega) = (\lambda(\omega), q_e(\omega), n(\omega))$ into another random vector

$\mathbf{v}(\omega) = (v_1(\omega), v_2(\omega), v_3(\omega))$ as follows

$$\begin{aligned} v_1 &= r_1(\lambda, q_\mathrm{e}, n) = t_\rho = \frac{\left(1 - \frac{\rho}{q_\mathrm{e}}\right)^{1-n} - 1}{\lambda(n-1)}, \\ v_2 &= r_2(\lambda, q_\mathrm{e}, n) = q_\mathrm{e}, \\ v_3 &= r_3(\lambda, q_\mathrm{e}, n) = n. \end{aligned}$$

are the deterministic one-to-one transformations $\mathbf{r} : \mathbb{R}^3 \to \mathbb{R}^3$ from $\mathbf{u}(\omega)$ to $\mathbf{v}(\omega) = (v_1(\omega), v_2(\omega), v_3(\omega))^\top$ random vector.
The inverse mapping $\mathbf{s} : \mathbb{R}^3 \to \mathbb{R}^3$ of $\mathbf{s}$ is

$$\begin{aligned} \lambda &= s_1(v_1, v_2, v_3) = \frac{\left(1 - \frac{\rho}{v_2}\right)^{1-v_3} - 1}{v_1(v_3 - 1)}, \\ q_\mathrm{e} &= s_2(v_1, v_2, v_3) = v_2, \\ n &= s_3(v_1, v_2, v_3) = v_3, \end{aligned}$$

and, by the above deductions (see Section 2.1), the inverse mapping is well-defined in the conditional probability space $(\Omega, \mathcal{F}_\Omega, \mathbb{P}[\cdot|C])$. Notice that, the absolute value of its Jacobian is

$$|J| = \left| -\frac{\left(1 - \frac{\rho}{v_2}\right)^{1-v_3} - 1}{v_1^2(v_3 - 1)} \right| = \frac{\left(1 - \frac{\rho}{v_2}\right)^{1-v_3} - 1}{v_1^2(v_3 - 1)} > 0.$$

Hence, by Th. 1 the joint PDF of $\mathbf{v}$ is given by

$$f_{v_1,v_2,v_3}(v_1, v_2, v_3) = f_0\left(\frac{\left(1 - \frac{\rho}{v_2}\right)^{1-v_3} - 1}{v_1(v_3 - 1)}, v_2, v_3\right) \frac{\left(1 - \frac{\rho}{v_2}\right)^{1-v_3} - 1}{v_1^2(v_3 - 1)}.$$

Finally, the PDF of the time $t_\rho(\omega)$ (ρ fixed) is

$$f_t(t_\rho) = \frac{1}{\mathbb{P}[C]} \int_\rho^\infty \int_1^\infty f_0 \left(\frac{\left(1 - \frac{\rho}{q_\mathrm{e}}\right)^{1-n} - 1}{t_\rho(n-1)}, q_\mathrm{e}, n \right) \frac{\left(1 - \frac{\rho}{q_\mathrm{e}}\right)^{1-n} - 1}{t_\rho^2(n-1)} \, \mathrm{d}n \, \mathrm{d}q_\mathrm{e}, \tag{14}$$

where

$$\mathbb{P}[C] = \int_\rho^\infty f_{q_\mathrm{e}}(q_\mathrm{e}) \, \mathrm{d}q_\mathrm{e}, \tag{15}$$

normalises the area under the curve to 1 so that the resulting function becomes a PDF. This expression is equivalent to integrate $q_\mathrm{e}(\omega)$ over its entire domain, but within the conditional probability space $(\Omega, \mathcal{F}_\Omega, \mathbb{P}[\cdot|C])$.

As before, if $\lambda(\omega)$, $n(\omega)$ and $q_\mathrm{e}(\omega)$ are independent, the PDF takes the following form

$$f_t(t_\rho) = \frac{1}{\mathbb{P}[C]} \int_\rho^\infty \int_1^\infty f_\lambda \left(\frac{\left(1 - \frac{\rho}{q_\mathrm{e}}\right)^{1-n} - 1}{t_\rho(n-1)} \right) f_{q_\mathrm{e}}(q_\mathrm{e}) f_n(n) \frac{\left(1 - \frac{\rho}{q_\mathrm{e}}\right)^{1-n} - 1}{t_\rho^2(n-1)} \, \mathrm{d}n \, \mathrm{d}q_\mathrm{e}.$$

As a particular case of the PDF of t_ρ, one of the most common applications in the systems analysis is the calculation of the so-called settling time, which we define as the time it takes for a system to reach a percentage p (for example, 50% or 95%) of the equilibrium value. However, in this model, the equilibrium quantity $q_\mathrm{e}(\omega)$ is a random variable, so we can take the expected value $\mathbb{E}[q_\mathrm{e}(\omega)]$ to obtain the PDF of the time t_ρ. If we establish that $\rho = p \, \mathbb{E}[q_\mathrm{e}(\omega)]$, then we obtain that

$$f_t(t_\rho) = \frac{1}{\mathbb{P}[C]} \int_\rho^\infty \int_1^\infty f_0 \left(\frac{\left(1 - p\frac{\mathbb{E}[q_\mathrm{e}(\omega)]}{q_\mathrm{e}}\right)^{1-n} - 1}{t_\rho(n-1)}, q_\mathrm{e}, n \right) \times \frac{\left(1 - p\frac{\mathbb{E}[q_\mathrm{e}(\omega)]}{q_\mathrm{e}}\right)^{1-n} - 1}{t_\rho^2(n-1)} \, \mathrm{d}n \, \mathrm{d}q_\mathrm{e}.$$

2.3 PDF of the rate coefficient, k_n, of the kinetic chemical reaction

As the rate coefficient, $k_n(\omega)$, of the PNO kinetic model (2)–(3) is a random variable, it is interesting to obtain its PDF. This can be achieved by applying Th. 1 with an appropriate mapping. With this aim, let us define $\mathbf{r} : \mathbb{R}^3 \to \mathbb{R}^3$, such that the random vector $\mathbf{u}(\omega) = (\lambda(\omega), q_\mathrm{e}(\omega), n(\omega))$ is transformed into $\mathbf{v}(\omega) = (v_1(\omega), v_2(\omega), v_3(\omega)) = (\lambda(\omega)/q_\mathrm{e}(\omega)^{n(\omega)-1}, q_\mathrm{e}(\omega), n(\omega))$, whose inverse mapping, $\mathbf{s} : \mathbb{R}^3 \to \mathbb{R}^3$, is given by

$$\begin{aligned} \lambda &= s_1(v_1, v_2, v_3) = v_1 v_2^{v_3-1}, \\ q_\mathrm{e} &= s_2(v_1, v_2, v_3) = v_2, \\ n &= s_3(v_1, v_2, v_3) = v_3. \end{aligned}$$

Observe that $\mathbf{s}$ is well-defined since all variables resulting from the transformation belong to its domain. On the other hand, the absolute value of its Jacobian is $|J| = v_2^{v_3-1} > 0$.
Notice that $v_1(\omega) := k_n(\omega)$, so, applying first Th. 1 and then marginalizing with respect to $v_2(\omega) := q_\mathrm{e}(\omega)$ and $v_3(\omega) := n(\omega)$, one obtains the PDF of $k_n(\omega)$

$$f_{k_n}(k_n) = \int_0^\infty \int_1^\infty f_0\left(k_n q_\mathrm{e}^{n-1}, q_\mathrm{e}, n\right) q_\mathrm{e}^{n-1} \,\mathrm{d}n \,\mathrm{d}q_\mathrm{e}. \tag{16}$$

3 An application

The stochastic PNO model has been applied on a data set available in a study about cadmium adsorption on tree fern, in which PSO models were applied [12]. The data are shown in Table 1. It should be noted that, although only 9 source data are available, the dynamics of the complete adsorption process up to equilibrium can be clearly appreciated. This section is aimed at applying our previous theoretical findings in a real-world chemistry setting.

To apply the theoretical results, it is first necessary to establish a joint

Time t_i (min)	**Adsorbed quantity q_i (mg/g)**
0	0
4	7.172414
5	8.022989
10	9.724138
15	9.793103
20	10.551724
30	10.574713
45	11.103448
60	11.195402

Table 1. Adsorption capacity of cadmium ions onto tree fern, q_i, for different time instants t_i, $i \in \{1, 2, \ldots, 9\}$. Source [12].

PDF of the model parameters. In this model, from a physical parameter perspective, the normalized equilibrium quantity q_e will depend mainly on the available adsorbent surface area (its geometry, binding sites, etc.), the normalized adsorption rate λ of the molecule, on the affinity between adsorbent and adsorbate molecules (and other factors that alter it, such as concentration, temperature, pH, etc.), and the order n, on the stoichiometric adsorbent-adsorbate ratio of the reaction. For these differing reasons for each parameter, we assume that the parameters are independent random variables, so that, $f_0(\lambda, q_\mathrm{e}, n) = f_\lambda(\lambda) f_{q_\mathrm{e}}(q_\mathrm{e}) f_n(n)$. Therefore, a marginal PDF must be assigned for each of the parameters. Finding appropriate parameter distributions that best capture the data uncertainty is a crucial step in practice. In this problem, we face this challenge by means of two different approaches: the RLMS (Random Least Mean Square) method, and the Bayesian method. Once adequate parameter distributions have been set, we can calculate the expectation of the solution at every time instant in Table 1 as well as confidence intervals using (7)–(8). Moreover, the goodness-of-fit of the method can be assessed by computing the RMSE and MAPE errors between the expected value and the data.

3.1 RLMS method

The RLMS method assumes that each of the model parameters follows a parametric probability distribution governed by optimal parameters, which

best fit the data to the expected value of the 1-PDF of the model solution, or equivalently, which minimises the LMS error between them. RLMS technique requires the assumption of specific parametric distributions for the model parameters. The choice of probability distributions for each parameter must be in accordance with its domain and the information available about it.

Since the adsorption rate parameter λ is positive, we will propose a Gamma distribution with shape parameter $\alpha > 0$ and scale parameter $\beta > 0$, i.e., $\lambda(\omega) \sim \mathrm{Ga}(\alpha, \beta)$. For the equilibrium quantity q_e, we will consider a Uniform distribution, i.e. $q_\mathrm{e}(\omega) \sim \mathrm{Unif}(a, b)$, with $a, b > 0$. Finally, for the parameter n, we will assume a truncated Normal distribution on the interval $T = [1, 3]$, i.e. $n(\omega) \sim \mathrm{N}_T(\mu, \sigma^2)$. The choice of the Normal distribution in this case is motivated by the fact that values close to 2 are the ones that work best for this type of problems according to the literature and, about the truncation, the order is required to be $n > 1$ (in our case study), and that $n > 3$ values have rarely been observed in other processes.

The choice of reasonable distributions is the critical point of the RLMS method for estimating model parameters, since diverse possibilities can be handled. This choice has been based on the significance of the parameters in the model, their positivity, their boundedness and the information available on them. However, the generality of the results presented above allows the choice of distinct probability distributions for the model parameters of those already chosen which can be seen as a major advantage from a practical standpoint.

To ascertain the 1-PDF of the solution, it is first necessary to determine the parameters of the proposed parametric distributions, $\alpha, \beta, a, b, \mu, \sigma$, since it depends on these parameters. To that end, we will minimize the MSE between the observed data, q_i, and the expectation of the solution $q(t_i, \omega; \alpha, \beta, a, b, \mu, \sigma)$ evaluated at the time instants t_i. This leads to the following optimization program:

$$\min_{a,b,\mu,\sigma,\alpha,\beta>0} \quad \sum_{i=1}^{9} \left(q_i - \mathbb{E}\left[q(t_i, \omega; \alpha, \beta, a, b, \mu, \sigma)\right]\right)^2, \tag{17}$$

where the values of q_i are collected in Table 1, and the expectation of the solution, $\mathbb{E}\left[q(t_i,\omega;\alpha,\beta,a,b,\mu,\sigma)\right]$, is computed by the equation (7) with $f_1(q,t)$ defined in (12), where the PDFs involved in this expression have the following explicit expressions:

$$f_\lambda\left(\frac{\left(1-\frac{q}{q_\mathrm{e}}\right)^{1-n}-1}{t(n-1)};\alpha,\beta\right)=\frac{1}{\Gamma(\alpha)\beta^\alpha}\left(\frac{\left(1-\frac{q}{q_\mathrm{e}}\right)^{1-n}-1}{t(n-1)}\right)^{\alpha-1}\mathrm{e}^{-\frac{\left(1-\frac{q}{q_\mathrm{e}}\right)^{1-n}-1}{\beta t(n-1)}},$$

$$f_{q_\mathrm{e}}\left(q_\mathrm{e};a,b\right)=\begin{cases}\frac{1}{b-a}, & q_\mathrm{e}\in[a,b],\\ 0, & \text{otherwise},\end{cases}\quad f_n\left(n;\mu,\sigma\right)=\begin{cases}\frac{1}{\sigma}\frac{\phi\left(\frac{n-\mu}{\sigma}\right)}{\phi\left(\frac{3-\mu}{\sigma}\right)-\phi\left(\frac{1-\mu}{\sigma}\right)}, & n\in[1,3],\\ 0, & \text{otherwise},\end{cases}$$

where, $\phi(x)=\frac{1}{\sqrt{2\pi}}\,\mathrm{e}^{-\frac{1}{2}x^2}$.

We compute the optimal values, we have used the Nelder-Mead's algorithm implemented in Mathematica© software. Now, we explain the steps followed to calculate them. To bound the search region of the parameters, we have previously applied a deterministic non-linear fit of the PNO equation to the data, obtaining the optimal point estimates of the parameters ($\lambda^*=0.406614$, $q_\mathrm{e}^*=11.4436$ and $n^*=1.85576$), and their standard errors ($\mathrm{SE}_{\lambda^*}=0.061970$, $\mathrm{SE}_{q_\mathrm{e}^*}=0.383105$ and $\mathrm{SE}_{n^*}=0.32279$). The parameters of the probability distributions of the three model parameters have then been found such that their expected values match the above optimal estimates, and their variance match the above squared standard errors, i.e,

$$\begin{aligned}
&\lambda\sim\mathrm{Ga}(\alpha_0,\beta_0):\quad \mathbb{E}[\lambda]=\lambda^*,\ \mathbb{V}[\lambda]=\mathrm{SE}_{\lambda^*}^2,\\
&q_\mathrm{e}\sim\mathrm{Unif}(a_0,b_0):\quad \mathbb{E}[q_\mathrm{e}]=q_\mathrm{e}^*,\ \mathbb{V}[q_\mathrm{e}]=\mathrm{SE}_{q_\mathrm{e}^*}^2,\\
&n\sim\mathrm{N}(\mu_0,\sigma_0):\quad \mathbb{E}[n]=n^*,\ \mathbb{V}[n]=\mathrm{SE}_{n^*}^2.
\end{aligned}$$

Finally, the local optimal search for parameters of the distributions using the Nelder Mead algorithm has been bounded around the values obtained $(\alpha_0,\beta_0,a_0,b_0,\mu_0,\sigma_0)$. The result of the minimisation problem (17) has been

$$\alpha=42.0172,\ \beta=0.009594,\ a=10.9934,\ b=12.1161,\ \mu=1.8858,\ \sigma=0.3710.$$

3.2 Bayesian method

From a Bayesian perspective, we will consider that the data sequence $\mathbf{q} = (q_1, \ldots, q_9)$ (whose values are strictly positive) come from a probability (or likelihood) distribution $f_{\mathbf{q}|\boldsymbol{\theta}}(\mathbf{q} \mid \boldsymbol{\theta})$, which depends on a set of random parameters $\boldsymbol{\theta}$ that follows a prior probability distribution $f_{\boldsymbol{\theta}}(\boldsymbol{\theta})$, constructed according to the prior information we have about these parameters (e.g., from experience published in the scientific literature). Formally,

$$\mathbf{q} \mid \boldsymbol{\theta} \sim f_{\mathbf{q}|\boldsymbol{\theta}}(\mathbf{q} \mid \boldsymbol{\theta}), \quad \boldsymbol{\theta} \sim f_{\boldsymbol{\theta}}(\boldsymbol{\theta}).$$

From this information, Bayes' theorem allows us to calculate the posterior distribution as

$$\begin{aligned} \boldsymbol{\theta} \mid \mathbf{q} &\sim f_{\boldsymbol{\theta}|\mathbf{q}}(\boldsymbol{\theta} \mid \mathbf{q}), \\ f_{\boldsymbol{\theta}|\mathbf{q}}(\boldsymbol{\theta} \mid \mathbf{q}) &= \frac{f_{\boldsymbol{\theta}}(\boldsymbol{\theta}) f_{\mathbf{q}|\boldsymbol{\theta}}(\mathbf{q} \mid \boldsymbol{\theta})}{\int_{\boldsymbol{\theta}} f_{\boldsymbol{\theta}}(\boldsymbol{\theta}) f_{\mathbf{q}|\boldsymbol{\theta}}(\mathbf{q} \mid \boldsymbol{\theta}) \, \mathrm{d}\boldsymbol{\theta}} \propto f_{\boldsymbol{\theta}}(\boldsymbol{\theta}) f_{\mathbf{q}|\boldsymbol{\theta}}(\mathbf{q} \mid \boldsymbol{\theta}). \end{aligned}$$

The posterior distribution can be interpreted as the prior distribution of the parameters updated with the information provided by the experimental data.

In our application, we define $\boldsymbol{\theta} = (\lambda, q_{\mathrm{e}}, n, \beta)$ considering that there is independence between the parameters, and we assume, also by independence, that each observation, q_i, in the data sequence, $\mathbf{q}$, follows a Gamma time-dependent distribution such that its rate parameter β is fixed over time, and its shape parameter α_i depends on the expected value, which is equal to the solution of the PNO model:

$$\begin{aligned} & q_i \mid (\lambda, q_{\mathrm{e}}, n, \beta) \sim \mathrm{Ga}(\alpha_i, \beta), \\ & \mathbb{E}[q_i \mid (\alpha_i, \beta)] = \frac{\alpha_i}{\beta} = q_{\mathrm{e}} - q_{\mathrm{e}} \left(\frac{1}{1 + (n-1)\lambda t_i} \right)^{\frac{1}{n-1}}, \\ & \alpha_i = \alpha_i(\lambda, q_{\mathrm{e}}, n, \beta) = \beta \left(q_{\mathrm{e}} - q_{\mathrm{e}} \left(\frac{1}{1 + (n-1)\lambda t_i} \right)^{\frac{1}{n-1}} \right). \end{aligned}$$

Subsequently, we shall compute suitable priori distributions for each of the model parameters. In the case of the parameters q_{e} and β, they have

been assigned non-informative prior distributions, with high variability. For q_e, a prior distribution Unif$(0, 100)$ has been taken, while for β a Ga$(0.01, 0.01)$ distribution has been chosen. However, for more sensitive model parameters, such as n and λ, it has been necessary to give them more informative distributions.

For the λ parameter, a total of 56 values have been collected from 5 research papers [10, 14–17] in which the adsorption of metal ions, such as Cd(II), Pb(II) or Cu(II) ions, under different conditions (temperature, pH, etc.) on plant substrate was modelled using PFO and PSO models. No generalised PNO models have been found in the analyzed literature for this particular application. The values of λ have been obtained from the k_n published values by using equation 3. For the n parameter, the search has been extended to adsorption processes in general modelled with the PNO model. A total of 23 values were taken from a review work [37].

Then, for each parameter, its cumulative empirical distribution has been calculated, and a deterministic nonlinear LMS fit has been made with three types of cumulative distribution functions: Log-Normal, Normal and Gamma. Between the three, the distribution with the lowest MSE has been chosen as the prior distribution. The `Scipy` Python library has been used for the fit. Table 2 and Figure 1 show the results of the fit. The results suggest that the Log-Normal distribution is the best fit to the available prior information, and is therefore the best candidate as the prior distribution for both λ and n. Additionally, the Log-Normal distribution for n has been truncated in the interval $T = [1, 3]$, since the model presents the $n > 1$ restriction, and values greater than 3 for n have not been observed in the prior information available.

Parameter	**Best** LN(μ, σ)	**Best** N(μ, σ)	**Best** Ga(α, β)
	LN$(-1.284, 0.826)$	N$(0.326, 0.286)$	Ga$(1.026, 2.626)$
λ	MSE = **0.000677**	MSE = 0.00107	MSE = 0.000796
	LN$(0.562, 0.437)$	N$(1.820, 0.727)$	Ga$(1.960, 0.951)$
n	MSE = **0.00218**	MSE = 0.00560	MSE = 0.0110

Table 2. Best prior distributions for λ and n resulting from non-linear fitting.

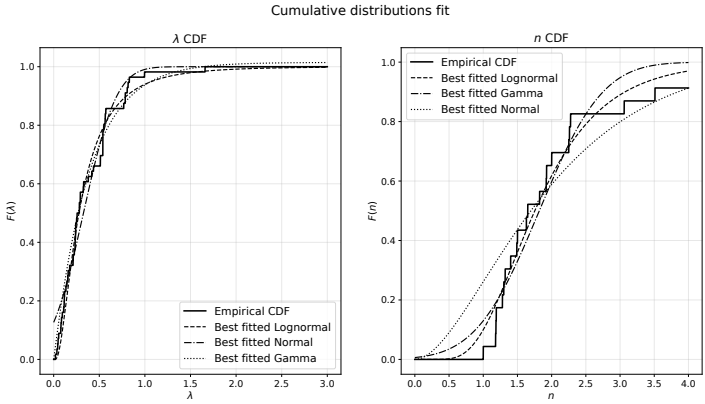

Figure 1. Best fit of Log-Normal, Normal and Gamma distributions to empirical cumulative prior distributions for λ and n parameters.

Therefore, the prior distributions of the parameters are given by

$$\begin{aligned}
\lambda &\sim \mathrm{LN}(-1.284, 1.465683),\\
q_{\mathrm{e}} &\sim \mathrm{Unif}(0, 100),\\
n &\sim \mathrm{LN}_T(0.562, 5.236452),\\
\beta &\sim \mathrm{Ga}(0.01, 0.01),
\end{aligned}$$

being $f_\lambda(\lambda), f_{q_{\mathrm{e}}}(q_{\mathrm{e}}), f_n(n)$ and $f_\beta(\beta)$ their respective PDFs, whose definitions can be found in Appendix D.

To calculate the posterior distribution, we have used the statistical software RStudio and WinBUGS. We have applied the `bugs` function of the `R2Winbugs` package of RStudio. This package interacts with Winbugs, which in turn works with an iterative algorithm called Gibbs sampling and Metropolis algorithm to solve the problems. The Markov chain resulting from this algorithm is a sample of the desired posterior distribution, since Markov Chain Monte Carlo (MCMC) simulation method consists of constructing a Markov chain that converges to a stationary distribution. The kernel density estimation method is then used to obtain the densities.

To evaluate the convergence of the MCMC chains constructed by the

above algorithm to its stationary process, we set 3 chains, where the starting values for the WinBUGS model are generated by the software itself, 300000 iterations for each chain, with 10% of the iterations as burn-in period, i.e. 30000, and with the argument `n.thin`=10, which means that the algorithm saves 1 value after 10 iterations. This is to avoid autocorrelation between values. Therefore, the resulting sample size for each chain is $N = 27000$. A visual representation of the convergence or lack thereof can be the trace plots, shown in Figure 5 (left column). They show the 3 chains well mixed with a random scatter around the mean value. In the same figure we can see the results of the deviance, a measure of fit calculated automatically by WinBUGS itself, and defined as $-2\log(\text{likelihood})$, where likelihood is the conditional probability of all data given the parameters.

The results obtained are the marginal posterior distributions of each parameter, which are also shown in Figure 5 (right column). The bandwidth values used for the kernel are shown in the same column. These values are used to smooth the samples and produce these density estimates. Finally, we have used the `coda` package to perform posterior analyses of the simulated values. These include the Gelman and Rubin's convergence diagnostic, whose potential scale reduction factor gave 1 for all estimated parameters, indicating that the MCMC sample converges to the estimate of the posterior distribution for each parameter.

3.3 Results and discussion

In this section we exhibit our main results based on the computation carried out using our theoretical findings in the setting of the model analyzed in the foregoing section.

In Figure 2, we show the 1-PDF, $f_1(q,t)$, of the solution, $q(t,\omega)$, using the RLMS and Bayesian methods explained in the previous subsection. In both plots, we observe that, for each time instant, the PDF is approximately concentrated around the recorded adsorbed amount, following a morphology very similar to the Gaussian one. It can also be seen that the mass of the density shifts with time towards amounts closer and closer to equilibrium levels, with a certain leptokurtic tendency. As differences, in

Figure 2a (RLMS), there is a certain negative skewness, while in Figure 2a (Bayesian), the distribution remains approximately symmetric.

On the other hand, in Figure 3 we show the expected value and 95%-confidence intervals. They have been calculated thanks to the previus computation of the 1-PDF according to (7)–(9). With respect to the expected value, we observe that, in both cases, they fit the data series well at all time instantants. The metrics of this fit, reflected in Table 4, indicate a very low and very similar error for the two methods, around 0.16 for the RMSE, and around $1.6\% - 1.7\%$ for the MAPE. With respect to the confidence intervals, we find that both methods capture all the data, and that the Bayesian method yields a slightly wider confidence region than the RLMS. Note also that, in the RLMS intervals, the aforementioned asymmetry of the upper confidence interval can be observed in full agreement with the plots shown in Figure 2.

Complementary, in Table 3, which includes the expected value, variance and 95%-confidence interval, it is shown how the evolution of the expected value is increasing with time and stabilises around equilibrium, while the variance is approximately stable with time. As a practical example of the usability of the model, we can state, for this chemisorption process and before running an equivalent experiment, that at the time instant $t = 7$ the amount adsorbed is expected to be 8.751 mg/g, with a confidence interval of $[7.28, 10.46]$.

Features of 1-PDF	$t=1$	$t=2$	$t=4$	$t=5$	$t=7$	$t=10$	$t=15$	$t=20$	$t=30$	$t=45$	$t=60$
$\mathbb{E}[q(t,\omega)]$	3.360	5.261	7.317	7.927	8.751	9.470	10.094	10.430	10.763	10.928	11.029
$\mathbb{V}[q(t,\omega)]$	0.175	0.360	0.585	0.642	0.661	0.621	0.521	0.430	0.445	1.156	1.371
Lower limit of 95%-CI	2.59	4.17	5.95	6.51	7.28	8.01	8.70	9.12	9.6	9.97	10.19
Upper limit of 95%-CI	4.23	6.54	8.95	9.63	10.46	11.07	11.48	11.66	11.81	11.9	11.94

Table 3. Values of the 1-PDF characteristics of the solution, such as the expectation, variance and the lower and upper limits of the 95%-CI (confidence intervals).

On the other hand, Figure 4 shows the PDF of the time, $t_\rho(\omega)$, required to reach a certain quantity ρ, using the RLMS and Bayesian methods. In both casess it is observed that, as the quantity, ρ, increases, the PDF becomes increasingly platicurtic. If we look at the numerical results shown in Table 5, we observe that both the expected value and the variance of the PDF of time grow with larger ρ quantities, indicating this platicurtic

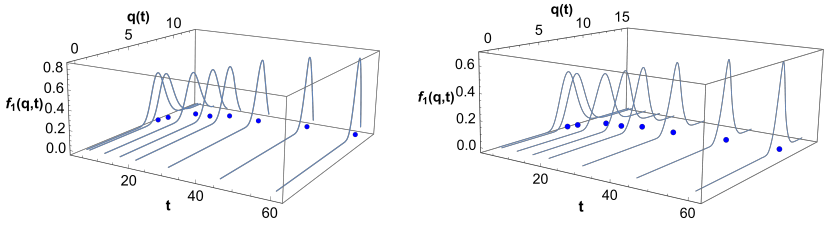

(a) RLMS approach **(b)** Bayesian approach

Figure 2. Visual representation of the 1-PDF of the solution of the random PNO model, $f_1(q,t)$, given in Eq. (12), at time instants t_i for $i = 2, ..., 9$, collected in Table 1.

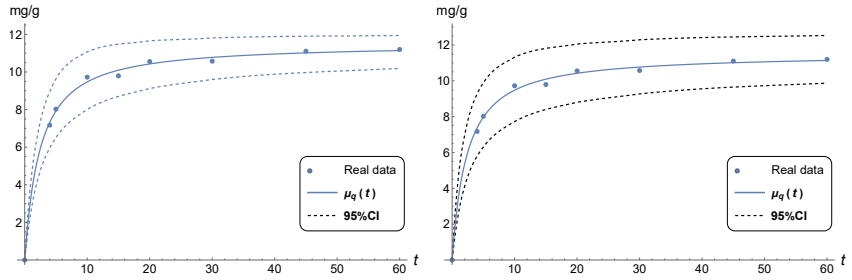

(a) RLMS approach **(b)** Bayesian approach

Figure 3. Plot of the expectation (solid line) together with the 95% confidence intervals (dashed lineas) of the solution stochastic process of the random PNO model, representing the probabilistic fit of the data (dots) specified in Table 1.

tendency. The statistics in Table 5 have been calculated as follows:

$$\mathbb{E}[t_\rho(\omega) \mid C] = \frac{\mathbb{E}[t_\rho(\omega)\mathbb{1}_C]}{\mathbb{P}[C]}, \quad \mathbb{V}[t_\rho(\omega) \mid C] = \frac{\mathbb{V}[t_\rho(\omega)\mathbb{1}_C]}{\mathbb{P}[C]}, \quad \omega \in \Omega,$$

where $\mathbb{1}_C$ is the characteristic function for the event C. Note that these values are computed on the conditional probability space $C = \{\omega \in \Omega : q_e > \rho\}$ (see Section 2.2), whose probability $\mathbb{P}[C]$, defined in the equation (15), is also shown in Table 5. In this case, for large values of ρ, it is reduced, since the equilibrium quantity q_e concentrates in its PDF (in both methods) most of the density in the interval $[10, 13]$.

After observing the results of the two methods, it could be inferred that, although both fit the expected value very similarly, the results of the

Measures \ Methods	RLMS	Bayesian
RMSE	0.167344	0.169611
MAPE (%)	1.66	1.68

Table 4. Comparison of goodness-of-fit measures (RMSE and MAPE) between the two approaches (RMLE and Bayesian) to determine model parameters PDFs of the random PNO model.

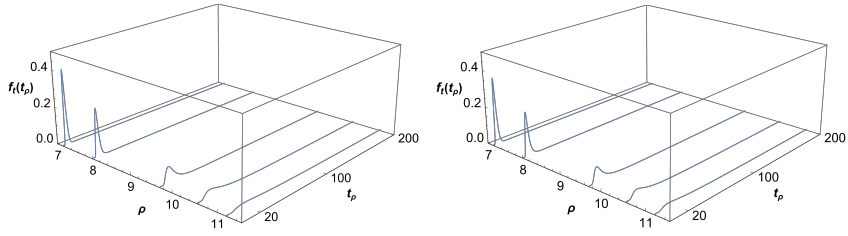

(a) RLMS approach **(b)** Bayesian approach

Figure 4. Time PDF for different fixed values of the adsorbed amount of reagent $\rho \in \{7.17241, 8.02299, 9.72414, 10.5747, 11.1954\}$. The results have been performed with the PDFs of the model parameters, λ, q_e and n, obtained from the two approaches, in the context of the PNO random model.

RLMS are slightly better and that its confidence interval is tighter, i.e. it has less uncertainty. However, it should be noted that the optimal parameters found for the RLMS using this specific data set do not necessarily return a good fit for other similar sets of experiments (by the definition of the minimisation problem (17)). Additionally, minimisation focuses on the expected value, but does not take into account the variance of the process, so there are potentially infinitely many optimal distributions (with an expected value fitted to the data) with multiple possible variances. In this case, we have chosen to restrict the variance to around the standard error of a deterministic fit, but it should be noted that, with a single data set, this approach may not be robust to setting confidence intervals. In contrast, the Bayesian method, while yielding greater uncertainty than the RLMS in its confidence interval, does incorporate information on the variance of the process within the prior distribution reported in the literature, and could therefore be considered more reliable than the RLMS method

		ρ				
		7.17241	8.02299	9.72414	10.5747	11.1954
RLMS approach	$\mathbb{P}[C]$	1	1	1	1	0.820077
	$\mathbb{E}[t_\rho(\omega)\|C]$	4.03714	5.60095	13.6152	31.2255	77.5207
	$\mathbb{V}[t_\rho(\omega)\|C]$	1.21461	3.27488	55.6106	743.916	10524.5
Bayesian approach	$\mathbb{P}[C]$	1	1	0.99995	0.99170	0.752903
	$\mathbb{E}[t_\rho(\omega)\|C]$	4.04707	5.70199	14.7011	35.0026	74.2476
	$\mathbb{V}[t_\rho(\omega)\|C]$	1.82789	5.31072	108.697	1480.63	11805.4

Table 5. Expectation and variance of the time needed to reach a given quantity of adsorbed amount.

in this respect.

On the other hand, regarding the results of the time needed to adsorb a quantity ρ, care must be taken when making estimates for large amounts of time. This is because, when the adsorbed amount is high, it is closer to equilibrium, there are many more time instants in which this amount has been (approximately) reached. Consequently, the probability distribution of time becomes increasingly flatter and less informative as ρ grows.

4 Conclusions

In this paper we have presented a methodology to analyze the pseudo-n order (PNO) model by treating all its model parameters, namely, rate coefficient, adsorption rate and order of the chemical reaction, as random variables with arbitrary distributions. Given real-world data, we have also shown two uncertainty quantifications techniques to assign appropriate distributions to all model parameters when applying the PNO equation to real-world data. To the best of our knowledge, this is the first time that this analysis is performed for the randomized PNO model, and we believe that the methodology can be very useful to perform chemical studies that want to account for the uncertainties that often are present in practice.

Appendices

A Proof of equivalence between Ritchie and PNO models

The Ritchie model is theoretically constructed from a molecular statistics perspective, considering that the surface is a lattice with $N_{\mathrm{e}} \in \mathbb{N}$ binding sites likely to be occupied, and that the adsorbed gas is a set of molecules, each of which occupies $n \in \mathbb{N}$ sites as it binds to the surface. If at an instant t, the number of occupied binding sites on the surface is $N(t)$, then

$$\theta(t) = \frac{N(t)}{N_e} \in \mathbb{Q}_{[0,1]},$$

where $\theta(t)$ represents the fraction of surface area occupied by the atoms of the adsorbed gas at time t. Furthermore, the model assumes that

- Adsorption is equally likely at all sites.
- There are no interactions between molecules.
- Adsorption is monolayer.
- There are no impurities (i.e. all molecules occupy the same number of n sites when adsorbing).

With all these considerations, if we assume that the variation of the occupied fraction $\theta(t)$ depends on the free fraction $1 - \theta$, then

$$\frac{d\theta(t)}{dt} = \lambda(1 - \theta(t))^n,$$

where λ (min^{-1}) is the adsorption rate. It should be noted that, although $\theta(t)$ is rational by definition, it can approximate a real value when the values of $N(t)$ and N_e are very high (in this case it is appropriate, since they represent the number of molecules).

On the other hand, the relationship between the number of occupied binding sites $N(t)$ and the adsorbed mass $q(t)$ (mg/g) is given by

$$q(t) = \frac{M_m}{N_{Av}} \frac{N(t)}{n} = CN(t),$$

where M_m (kg/mol) is the molecular mass of the adsorbed gas, $N_{Av} = 6.022 \times 10^{23}$ (1/mol) is the Avogadro number (particles/mol) and the number of adsorbed molecules is given by $\frac{N(t)}{n}$. Note that, at the end, the mass $q(t)$ is proportional to the number of molecules $N(t)$. From this relation it follows that

$$\theta(t) = \frac{N(t)}{N_{\mathrm{e}}} = \frac{CN(t)}{CN_{\mathrm{e}}} = \frac{q(t)}{q_{\mathrm{e}}}, \tag{18}$$

where q_{e} is the equilibrium mass quantity (for $t \to \infty$). Finally, taking the differential equation of Ritchie's model, and developing θ, we obtain that

$$\begin{aligned}
\frac{d\theta(t)}{dt} &= \lambda(1-\theta(t))^n, \\
\frac{d}{dt}\left(\frac{N(t)}{N_e}\right) &= \lambda\left(\frac{N_e - N(t)}{N_e}\right)^n, \\
\frac{d}{dt}\left(\frac{q(t)}{q_{\mathrm{e}}}\right) &= \lambda\left(\frac{q_{\mathrm{e}} - q(t)}{q_{\mathrm{e}}}\right)^n, \\
\frac{dq(t)}{dt} &= \frac{\lambda}{q_{\mathrm{e}}^{n-1}}\left(q_{\mathrm{e}} - q(t)\right)^n, \\
\frac{dq(t)}{dt} &= k_n\left(q_{\mathrm{e}} - q(t)\right)^n,
\end{aligned}$$

where

$$k_n = \frac{\lambda}{q_{\mathrm{e}}^{n-1}},$$

is the PNO adsorption rate. It is thus demonstrated that both models are the same, formulated in two different ways.

B Justification of the PNO model parameter domains

In the PNO model we find three parameters: λ, q_e and n.

Regarding the λ parameter, it is a ratio that regulates an adsorption process in which the fraction occupied by the adsorbate increases with time (desorption is not considered in this model). For this reason, the variation of the occupied fraction $\theta(t)$ with time (i.e. the derivative), must be positive, regardless of whether this variation is larger or smaller. From another point of view, λ can also be considered to represent the new fraction of area occupied per unit of time. Therefore, it must be fulfilled that $\lambda \in \mathbb{R}_{>0}$. And about q_e parameter, it is immediate that, since it is a mass quantity (specifically in equilibrium), it must be positive, i.e, $q_e \in \mathbb{R}_{>0}$.

About the n parameter, it represents in Ritchie's model the number of binding sites occupied by a molecule when it binds to the surface. It should therefore be considered as a discrete natural number. However, in reality, molecules do not all bind identically, using the same number of binding sites, so n can be relaxed and considered as the average number of binding sites of all molecules, allowing it to be a continuous parameter in $\mathbb{R}_{\geq 1}$. It should be noted that, for values of $n \in [0, 1)$, the model is no longer consistent from two approaches:

1. Physically, at the molecular level, the minimum lattice surface unit represents a binding site whereby a free molecule binds to another molecule on the surface, forming a chemical bond. In terms of a chemisorption reaction, it does not make sense for one molecule to partially react with another, and for the chemical bond to remain half-formed (bonding either occurs or does not occur). It could be theorised that there are weak molecular interactions (such as dipole-dipole or van der Waals forces) that partially or weakly bind molecules to the surface, and that an order $n < 1$ would represent these types of weak bonds. However, it should be remembered that any intermolecular interaction has been considered as non-existent

or negligible in this model. And even omitting such an assumption, assuming that all or most of the molecular bonds in the adsorption process were weak interactions would definitely indicate that we would not be dealing with a chemical adsorption process, but with others, such as diffusion.

2. Mathematically, if $n \in [0, 1)$, the general solution of the PNO equation reaches (from a certain instant of time) physically impossible adsorbed quantities. Knowing that

$$q(t) = q_{\mathrm{e}} - q_{\mathrm{e}} \left(\frac{1}{1 + (n-1)\lambda t} \right)^{\frac{1}{n-1}} \geq 0,$$

one derives that

$$(1 + (n-1)\lambda t)^{\frac{1}{1-n}} \leq 1. \tag{19}$$

If $n > 1$, then condition (19) is satisfied $\forall t > 0$, while if $n \in [0, 1)$, then it will only be satisfied for time instants t such that they satisfy the condition

$$1 + (n-1)\lambda t = 1 - (1-n)\lambda t > 0.$$

Therefore, for $q(t)$ to be defined in the reals, then

$$t < \frac{1}{\lambda(1-n)}.$$

For values of t that do not satisfy this condition, the solution will become complex. Consequently, the model makes no physical sense when $n < 1$, since in an adsorption process, the quantity $q(t)$ must be a real quantity at any instant of time.

Then, it can be stated that $\lambda \in \mathbb{R}_{>0}$, $q_{\mathrm{e}} \in \mathbb{R}_{>0}$ and $n \in \mathbb{R}_{\geq 1}$.

C Additional figures

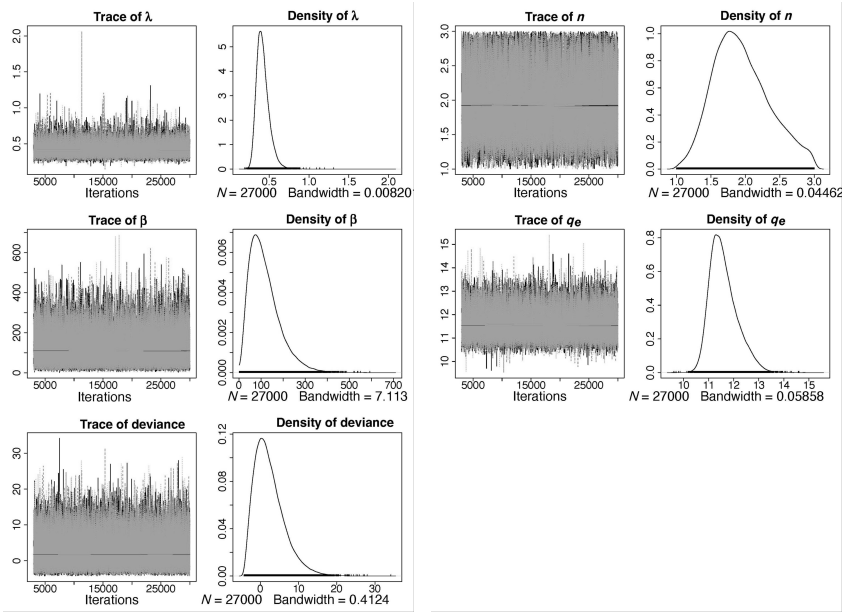

Figure 5. MCMC trace plots (left column) and marginal posterior distributions (right column) of the model parameters.

D Distributions

Log-Normal distribution used by WinBUGS

$$X \sim \mathrm{LN}(\mu, \tau) \qquad f_X(x; \mu, \tau) = \sqrt{\frac{\tau}{2\pi}} \frac{1}{x} e^{-\frac{\tau}{2}(\log x - \mu)^2}, \quad x > 0.$$

Log-Normal distribution

$$Y = e^X \sim \mathrm{LN}(\mu_x, \sigma_x), \quad \text{where} \quad X \sim \mathrm{N}(\mu_x, \sigma_x),$$

$$f_X(x; \mu, \sigma) = \frac{1}{\sigma\sqrt{2\pi}} \frac{1}{x} e^{-\frac{(\ln x - \mu)^2}{2\sigma^2}}, \quad x > 0.$$

It follows from these two distributions that $\tau = \frac{1}{\sigma^2}$.

Uniform distribution

$$X \sim \text{Unif}(a, b) \qquad f_X(x; a, b) = \frac{1}{b-a}, \quad a < x < b.$$

Gamma distribution used by WinBUGS

$$X \sim \text{Ga}(r, \mu) \qquad f_X(x; r, \mu) = \frac{\mu^r x^{r-1} e^{-\mu x}}{\Gamma(r)}, \quad x > 0.$$

***Acknowledgment*:** This work has been partially supported by the Spanish Ministerio de Economía, Industria y Competitividad (MINECO), the Agencia Estatal de Investigación (AEI) and Fondo Europeo de Desarrollo Regional (FEDER UE) grant PID2020–115270GB–I00, the Generalitat Valenciana (grant AICO/2021/302), el Fondo Social Europeo y la Iniciativa de Empleo Juvenil EDGJID/2021/185 and la ayuda PRE2021-101090, financiado por MCIN/AEI/10.13039/501100011033 y por el FSE+.

References

[1] N. A. Akbar, N. A. F. Kamil, N. S. Md. Zin, M. N. Adlan, H. A. Aziz, Assessment of kinetic models on Fe adsorption in groundwater using high-quality limestone, *IOP Conf. Ser. Earth Environ. Sci.* **140** (2018) #012030.

[2] I. Ali, V. K. Gupka, Advances in water treatment by adsorption technology, *Nat. Protoc.* **1** (2006) 2661–2667.

[3] E. Allen, *Modeling with Itô Stochastic Differential Equations*, Springer, New York, 2007.

[4] C. W. Cheung, J. F. Porter, G. McKay, Elovich equation and modified second-order equation for sorption of cadmium ions onto bone char, *J. Chem. Techn. Biotechn.* **75** (2000) 963–970.

[5] S. H. Chien, W. R. Clayton, Application of Elovich equation to the kinetics of phosphate release and sorption in soils, *Soil Sci. Soc. Am. J.* **44** (1980) 265–268.

[6] A. Dabrowski, Adsorption—from theory to practice, *Adv. Colloid Interface Sci.* **93** (2001) 135–224.

[7] G. L. Dotto, G. McKay, Current scenario and challenges in adsorption for water treatment, *J. Environ. Chem. Eng.* **8** (2020) #103988.

[8] S. D. Faust, O. M. Aly, *Adsorption Processes for Water Treatment*, Butterworth–Heinemann, Boston, 1987.

[9] V. K. Garg, M. Amita, R. Kumar, R. Gupta, Basic dye (methylene blue) removal from simulated wastewater by adsorption using Indian Rosewood sawdust: a timber industry waste, *Dyes Pigm.* **63** (2004) 243–250.

[10] I. Ghodbane, L. Nouri, O. Hamdaoui, M. Chiha, Kinetic and equilibrium study for the sorption of cadmium (II) ions from aqueous phase by eucalyptus bark, *J. Hazard. Mater.* **152** (2008) 148–158.

[11] B. E. Heyden, A. M. Bradshaw, The adsorption of CO on Pt (111) studied by infrared-reflection-adsorption spectroscopy, in: C. R. Brundle, H. Morawitz (Eds.), *Vibrations at Surfaces*, Elsevier, Amsterdam, 1983, pp. 51–51.

[12] Y. S. Ho, Second-order kinetic model for the sorption of cadmium onto tree fern: A comparison of linear and non-linear methods, *Water Res.* **40** (2006) 119–125.

[13] Y. S. Ho, G. McKay, Sorption of dye from aqueous solution by peat, *Chem. Eng. J.* **70** (1998) 115–124.

[14] Y. S. Ho, Removal of copper ions from aqueous solution by tree fern, *Water Res.* **37** (2003) 2323–2330.

[15] Y. S. Ho, Effect of pH on lead removal from water using tree fern as the sorbent, *Bioresour. Techn.* **96** (2005) 1292–1296.

[16] Y. S. Ho, W. T. Chiu, C. S. Hsu, C. T. Huang, Sorption of lead ions from aqueous solution using tree fern as a sorbent, *Hydrometallurgy* **73** (2004) 55–61.

[17] Y. S. Ho, C. C. Wang, Pseudo-isotherms for the sorption of cadmium ion onto tree fern, *Process Biochem.* **39** (2004) 761–765.

[18] S. Lagergren, *Zur theorie der sogenannten adsorption geloster stoffe*, Kungliga Svenska Vetenskapsakademiens, Handlingar, 1898.

[19] I. Langmuir, The adsorption of gases on plane surfaces of glass, mica and platinum, *J. Am. Chem. Soc.* **40** (1918) 1361–1403.

[20] G. Lefèvre, In situ Fourier-transform infrared spectroscopy studies of inorganic ions adsorption on metal oxides and hydroxides, *Adv. Colloid Interface Sci.* **107** (2004) 109–123.

[21] W. R. Lim, S. W. Kim, C. H. Lee, E. K. Choi, M. H. Oh, S. N. Seo, H. J. Park, S. Y. Hamm, Performance of composite mineral adsorbents for removing Cu, Cd, and Pb ions from polluted water, *Sci. Rep.* **9** (2019) 1–10.

[22] É. C. Lima, M. A. Adebayo, F. M. Machado, Kinetic and equilibrium models of adsorption, in: C. Bergmann, F. Machado, (Eds.) *Carbon Nanomaterials as Adsorbents for Environmental and Biological Applications*, Springer, Cham, 2015, pp. 33–69.

[23] M. J. D. Low, Kinetics of chemisorption of gases on solids, *Chem. Rev.* **60** (1960) 267–312.

[24] M. Majdan, O. Maryuk, S. Pikus, E. Olszewska, R. Kwiatkowski, H. Skrzypek, Equilibrium, FTIR, scanning electron microscopy and small wide angle X-ray scattering studies of chromates adsorption on modified bentonite, *J. Mol. Struct.* **740** (2005) 203–211.

[25] B. S. Marques, T. S. Frantz, T. R. Sant'Anna Cadaval Junior, L. A. de Almeida Pinto, G. L. Dotto, Adsorption of a textile dye onto piaçava fibers: kinetic, equilibrium, thermodynamics, and application in simulated effluents, *Environ. Sci. Pollut. Res.* **26** (2019) 28584–28592.

[26] H. Moussout, H. Ahlafi, M. Aazza, H. Maghat, Critical of linear and nonlinear equations of pseudo-first order and pseudo-second order kinetic models, *Karbala Int. J. Mod. Sci.* **4** (2018) 244–254.

[27] J. P. Muscat, D. M. Newns, Chemisorption on metals, *Prog. Surf. Sci.* **9** (1978) 1–43.

[28] A. Özer, Removal of Pb (II) ions from aqueous solutions by sulphuric acid-treated wheat bran, *J. Hazard. Mater.* **141** (2007) 753–761.

[29] E. Piperopoulos, L. Calabrese, E. Mastronardo, C. Milone, E. Proverbio, 8 - Carbon-based sponges for oil spill recovery, in: A. Kamel, Abd-Elsalam (Eds.), *Carbon Nanomaterials for Agri-food and Environmental Applications*, Elsevier, Amsterdam, 2020, pp. 155–175.

[30] A. Politano, G. Chiarello, G. Benedek, E. V. Chulkov, P. M. Echenique, Vibrational spectroscopy and theory of alkali metal adsorption and co-adsorption on single-crystal surfaces, *Surf. Sci. Rep.* **68** (2013) 305–389.

[31] H. Qiu, L. Lv, B.c. Pan, Q.j. Zhang, W.m. Zhang, Q.x. Zhang, Critical review in adsorption kinetic models, *J. Zhejiang Univ. Sci.* **10** (2009) 716–724.

[32] A. G. Ritchie, Alternative to the Elovich equation for the kinetics of adsorption of gases on solids, *Faraday Trans.* **73** (1977) 1650–1653.

[33] S. Rodríguez-Narciso, J. A. Lozano-Álvarez, R. Salinas-Gutiérrez, N. Castañeda-Leyva, A stochastic model for adsorption kinetics, *Adsorpt. Sci. Techn.* **2021** (2021) #5522581.

[34] R. C. Smith, *Uncertainty Quantification: Theory, Implementation, and Applications*, SIAM, New York, 2014.

[35] T. T. Soong, *Random Differential Equations in Science and Engineering*, Academic Press, New York, 1973.

[36] Z. Q. Tian, B. Ren, Adsorption and reaction at electrochemical interfaces as probed by surface-enhanced Raman spectroscopy, *Ann. Rev. Phys. Chem.* **55** (2004) 197–229.

[37] J. Wang, X. Guo, Adsorption kinetic models: Physical meanings, applications, and solving methods, *J. Hazard. Mater.* **390** (2020) #122156.

[38] Y. Zha, Y. Wang, S. Liu, S. Liu, Y. Yang, H. Jiang, Y. Zhang, L. Qi, H. Wang, Adsorption characteristics of organics in the effluent of ultrashort SRT wastewater treatment by single-walled, multi-walled, and graphitized multi-walled carbon nanotubes, *Sci. Rep.* **8** (2018) #17245.